

FOREST ECOSYSTEM PROCESSES AT THE WATERSHED SCALE: DYNAMIC COUPLING OF DISTRIBUTED HYDROLOGY AND CANOPY GROWTH

D. SCOTT MACKAY^{1*} AND LAWRENCE E. BAND²

¹*Department of Forest Ecology and Management and Institute for Environmental Studies, University of Wisconsin, Wisconsin, USA*

²*Department of Geography, University of Toronto, Canada*

ABSTRACT

The hydrological recovery of watersheds from disturbances such as fire and harvest can change the magnitude and distribution of flow paths as the canopy regenerates. The spatial distribution of net water input to the soil–topography system is mediated by vegetation patterns through the processes of interception, evapotranspiration and snowmelt. We have previously described RHESSys, a distributed model of water and carbon flux with a prescribed canopy cover. Although the canopy structure varied spatially it did not change through time. We present an expanded model in which carbon and nitrogen are dynamically coupled with distributed hydrology. The model fixes and allocates canopy carbon annually to reflect changes in climate forcing. We test the interactions of the forest ecosystem to distributed hydrology through controlled experiments. In the first experiment, we prescribe canopy cover and examine the sensitivity of the hydrological outputs to the distribution of vegetation. The canopy distribution is found to have significant effects on simulated hydrological outputs where evaporative demand exceeds available water. In a second experiment we simulate the canopy leaf area index (LAI) across the topography and through time. The model is executed over 100 years using repeated 10-year meteorological records to investigate spatial and temporal patterns of LAI. Annual precipitation and temperature differences result in temporally fluctuating LAI about a reasonably stable long-term mean. The topographical position has a strong effect on local forest canopy characteristics. As expected, simulated ecosystem processes are found to be sensitive to rooting depth in more water limited environments. © 1997 by John Wiley & Sons, Ltd.

Hydrol. Process., Vol. 11, 1197–1217 (1997).

(No. of Figures: 12 No. of Tables: 2 No. of Refs: 31)

KEY WORDS TOPMODEL; RHESSys; forest growth; LAI

INTRODUCTION

Non-destructive exploration of the potential effects of forest harvest, fire, flooding and other disturbances on watershed-scale hydrological processes, as well as on rates of recovery from disturbance, require models that capture the spatial distribution of vegetation–soil water linkages. This paper examines the interactions of spatial patterns of hydrological and forest ecosystem processes through the use of a distributed hydro-ecological model. Two important controls on the hydrological response of a watershed are the spatial patterns and interactions of water routing and vegetation. Routing influences the spatial distribution of soil moisture, the areal extent of saturated regions in the watershed and the timing of runoff. Vegetation influences the net loading of water to the soil by intercepting precipitation, some of which is directly evaporated, attenuating radiation interception to the snowpack and forest floor, and controlling the rate of evapotranspiration. Thus the spatial distribution of vegetation affects the magnitude and patterns for specific catchment water sources. In turn, flow paths distribute water from these sources and influence the spatial patterns of soil moisture required by the vegetation canopy to maintain cell turgor and by soil organisms to mineralize nutrients.

* Correspondence to: D. Scott Mackay.

Two vegetation variables, leaf area index (LAI) and rooting depth, are examined with the aim of determining how their spatial distribution affects the interaction between ecosystem physiological and hydrological processes. Band (1993) and Quinn *et al.* (1995) examined the effects of distributed vs. lumped representations of canopy and rooting depths to areally averaged watershed evapotranspiration, and found significant effects under certain conditions. LAI and rooting depth are often prescribed, as opposed to simulated, variables in hydrological models that attempt to incorporate a vegetation canopy (e.g. Band *et al.*, 1993; Wigmosta *et al.*, 1994) although Vertessy *et al.* (1996) have recently incorporated a fully distributed forest growth model into the TOPOG framework for application in small catchments. In the absence of an impermeable layer in the soil, the rooting zone depth is determined by species type and available soil water and nutrient content (Larcher, 1995), but is very difficult to observe at the landscape level. LAI can be estimated at large spatial scales from remotely sensed vegetation indices correlated with field LAI measurements. However, for predicting the recovery of a watershed from disturbance we cannot rely on prescribed LAI, but need to model its recovery across terrain with varying water and nutrient supply. In the next section we present our modelling framework, including spatial data representation and vegetation–hydrology coupling. We then describe a set of simulation experiments designed to investigate the specific interactions.

MODELLING FRAMEWORK

Spatial data processing

RHESSys (regional hydroecological simulation system) is a spatial data processing and simulation modelling environment for watershed-to-regional-scale water, carbon and nutrient flux (Running *et al.*, 1989; Band *et al.*, 1991, 1993; Nemani *et al.*, 1993). A summary of the RHESSys structure is provided in Figure 1. The distinguishing features of RHESSys are its tightly integrated spatial data processing and simulation modelling components. Processes are extrapolated to a larger region by some method of

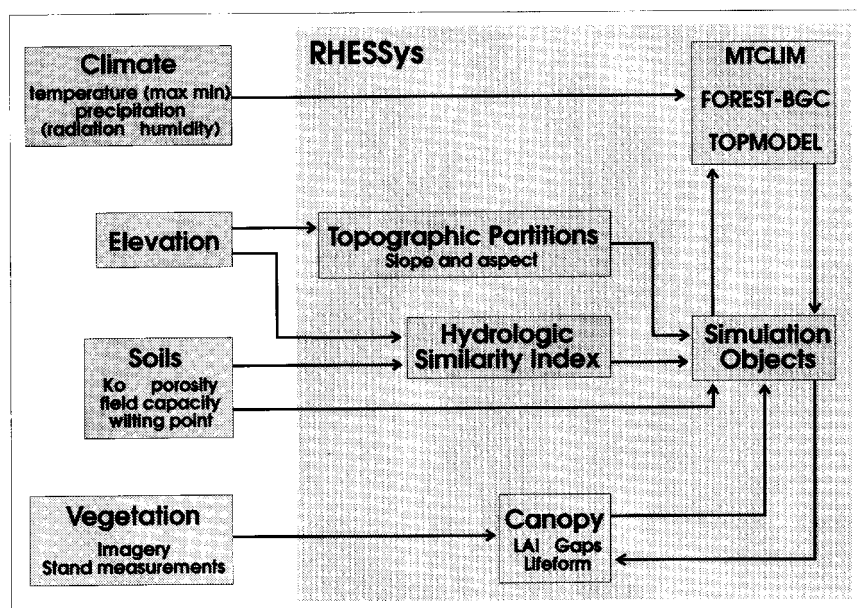


Figure 1. Overview of RHESSys, showing the spatial partitioning, wetness intervals and canopy structure components. Conceptually, RHESSys simulation objects capture landscape structural (Form) properties and processes (Function)

segmenting the landscape into relatively homogeneous regions with respect to one or more driving variables, then incorporating internal variation of other driving variables when expected values for these variables do not capture extreme conditions. For example, in mountainous areas RHESSys partitions the landscape into hillslope units that preserve between-partition variation in incident short-wave radiation (Band *et al.*, 1991); it then incorporates a joint distribution of vegetation, soils and topography to capture higher frequency responses of vegetation to the distribution of soil moisture (Band *et al.*, 1993). Other partitioning strategies include life form stands instead of hillslopes (Band, 1993), or a combination of lakes, wetlands and hillslopes (Mackay and Band, 1994). A three-tiered hierarchy that incorporates elevation zones as an intermediate level of spatial partitioning between hillslope and wetness intervals cocaptures within-hillslope adiabatic temperature lapse rates, which may account for differences in snowmelt timing from the ridge to stream within each hillslope. TOPMODEL (Beven and Kirkby, 1979) wetness intervals are then incorporated within each elevation zone within each hillslope.

The RHESSys framework provides the benefit of conceptually grouping areas in the landscape according to specific environmental controls on their behaviour. It also provides an efficient computational strategy for simulating large regions over long periods of time. The combined spatial data management and process-based modelling can either represent a landscape as a parallel set of independent units or as a series of interacting units (e.g. land–lake interaction). RHESSys integrates FOREST–BGC (Running and Coughlan, 1988) and TOPMODEL (Beven and Kirkby, 1979), a conceptual model of topographic and soil controls on the spatial distribution of the perched water tables. In addition, a climate simulator, MT–CLIM (Running *et al.*, 1987), extrapolates daily site-specific meteorological conditions (temperature, radiation, precipitation and humidity) on the basis of local elevation, slope and aspect from base station observations.

Vegetation–hydrology covariation

The hydrological model computes a local saturation deficit, which is the depth of water needed to bring the local perched water table to the ground surface, relative to a hillslope average saturation deficit. The local saturation deficit is given by

$$S_i = \bar{S} - m\{\chi_i - \lambda\} \quad (1)$$

where $\chi_i = \ln(aT_e/T_i \tan \beta)$ is the local topography–soils wetness index, which describes the relative amount of water at a given point with respect to the hillslope mean wetness index, λ . S_i and \bar{S} are local and hillslope mean saturation deficits, and m is a parameter that describes the rate of decay of saturated hydraulic conductivity with depth through the soil profile. Full derivation of this quasi-distributed hydrology is given by Beven (1986) and Sivapalan *et al.* (1987). The terms a (area drained per unit contour width) and $\tan \beta$ (local slope) are computed using terrain analysis derived from Band (1989), Wolock *et al.* (1989), Freeman (1991) and Quinn *et al.* (1991), and the spatial distribution of local soil transmissivities (T^i) and areally averaged transmissivity (T_e) are obtained from soils data. All areas within a given hillslope have the same χ values are conceptually viewed as hydrologically equivalent. A hillslope is thus represented by a set of intervals each characterizing a relative wetness with respect to each other and the hillslope mean. RHESSys assigns each interval the mean values of vegetation properties such as LAI and rooting depth. Typically, mean LAI for each interval has been determined with remote sensing techniques (Nemani *et al.*, 1993). Rooting depths are based on knowledge of life form and general soil properties and are considered quite uncertain. Within RHESSys, FOREST–BGC is operated on each interval (Figure 2) to maintain the local water balance and compute daily net canopy photosynthesis and nutrient cycling.

FOREST–BGC comprises a set of ‘big-leaf’ forest canopy physiology models that control the daily rate of evapotranspiration and carbon assimilation. The forest canopy controls the net water load on the soil–topography system by intercepting and evaporating rain and snow directly from the canopy and forest floor, by transpiration of soil water in the rooting zone and by regulating radiation exchange with the snowpack

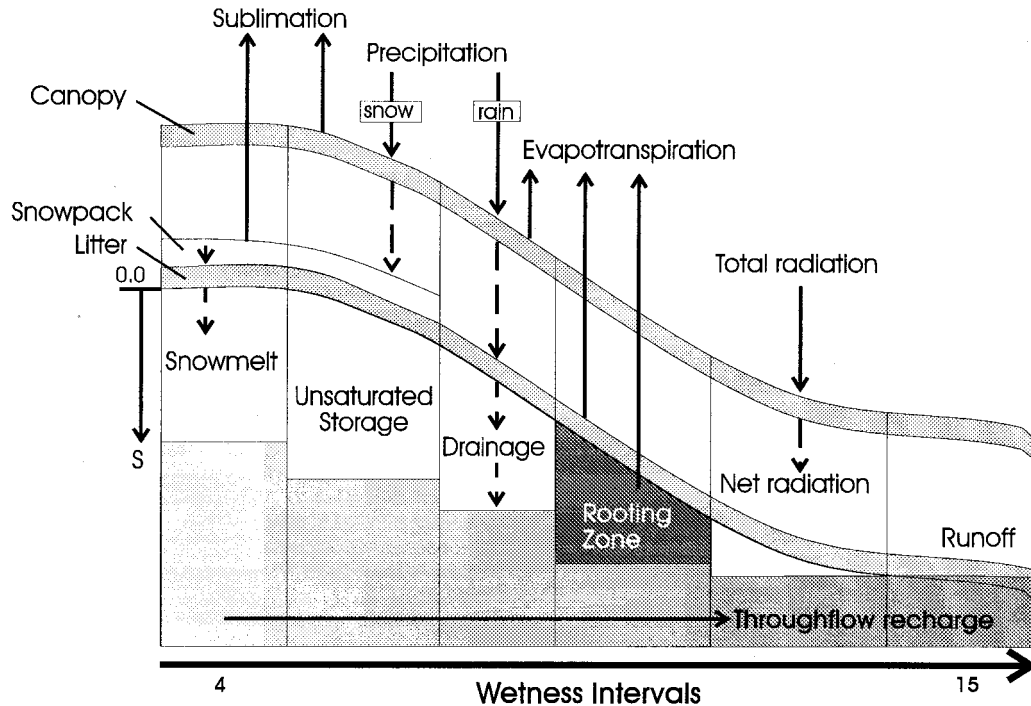


Figure 2. A full water balance is maintained within each interval over the distribution of the wetness index

on the forest floor. Transpiration (mm) is computed daily using the Penman–Monteith (Monteith, 1965) combination equation

$$t = \left\{ \frac{A_c \Delta + C_p \rho VPD G_a}{\rho_w LE (\Delta + \gamma (1 + G_a / G_c))} \right\} DAYL \quad (2)$$

where A_c is net canopy absorbed radiation (Wm^{-2}), Δ is the slope of the saturation vapour pressure–temperature curve ($\text{mbar } ^\circ\text{C}^{-1}$), C_p is specific heat capacity of air ($\text{J kg}^{-1} ^\circ\text{C}^{-1}$), ρ is the density of air, ρ_w is the density of water, γ is the psychrometric constant, VPD is vapour pressure at the air temperature (mbar), G_a is bulk vegetation aerodynamic conductance (m s^{-1}), LE is the latent heat of evaporation (J kg^{-1}), G_c is total canopy conductance (m s^{-1}) and $DAYL$ (s) is day length. G_c is assumed to be the canopy integration of average leaf level stomatal conductances as

$$G_c = \int_0^{\Lambda_T} g_s(\xi) d\xi \quad (3)$$

where Λ_T is total canopy LAI, $d\xi$ is an element of LAI and g_s is leaf level stomatal conductance. The daily value of g_s is a function of species-specific maximum stomatal conductance, predawn leaf water potential, minimum night temperature, humidity deficit and average absorbed radiation per unit LAI. Canopy total short-wave radiation is computed from total daily incident radiation using a Beer–Lambert formulation.

$$Q_A = Q_I (1 - \alpha_C) (1 - 0 - e^{-k\Lambda_P}) \quad (4)$$

where α_C is canopy albedo, k is a species-specific light extinction coefficient, Λ_P is projected LAI and Q_I is incident short-wave radiation at the top of the canopy. Short-wave radiation absorbed by the canopy is first

used to evaporate water stored on the canopy from interception. The energy used to evaporate water from the canopy is deducted from Q_A to obtain A_c , which is used in the Penman–Monteith combination equation to transpire water. Unevaporated water drips from the canopy and recharges litter interception storage on rain days, or snowpack on snow days. The PAR (photosynthetically active radiation) component of the remaining short-wave radiation proportion (after evaporation) is available to compute gross photosynthesis. Litter water storage is evaporated as a function of daily humidity deficits. In summer dry regions such as Onion Creek, litter interception of canopy throughfall can effectively reduce mineral soil recharge and runoff to negligible amounts.

Snowmelt follows a degree-day accumulation for snowpack ripening, with temperature and radiation melt processes. Both short-wave and long-wave radiation are used to melt the snowpack, although a full energy budget is currently not solved. Calculation of long-wave radiation is based on Linacre (1992). Sublimation is taken from unripened snowpack, using a fraction of the short-wave radiation that reaches the snowpack, on days when the air temperature is below freezing.

Rooting zone water limitations on stomatal physiology are quantified by calculation of the predawn leaf water potential (Ψ_L). Ψ_L is estimated as the soil water potential, Ψ_S , which, in turn, is a non-linear characteristic function of daily rooting zone and field capacity soil moisture contents. Predawn leaf water potential modifies maximum stomatal conductance of the leaves as

$$g_s = g_{s_{\max}} \left\{ 1 - \frac{(\Psi_L - \Psi_M)}{(\Psi_{SC} - \Psi_M)} \right\} \quad (5)$$

where Ψ_M and Ψ_{SC} , are spring minimum and stomatal closure leaf water potentials, respectively. Available rooting zone soil water is the total of the water in the unsaturated zone above the wilting point within the rooting zone and water in any saturated soil within the rooting zone. Drainage from the unsaturated soil zone to the saturated soil zone occurs at soil water contents between saturation and field capacity at a fraction of saturated hydraulic conductivity, as presented in Band *et al.* (1993). Once active drainage has stopped, further reduction of the unsaturated zone soil moisture to wilting point occurs through transpiration. In any areas where the whole rooting zone is unsaturated and at wilting point, stomatal closure occurs and transpiration ceases. The current model structure computes an average moisture content based on total available water, which is used to compute the soil water potential. This approach has the potential for overestimating transpiration rates in water-limited environments when only a small fraction of the rooting zone is saturated and the unsaturated portion has a high water potential, as the actual root surface area exposed to available water would be low. However, since the current model does not compute capillary rise it is also possible that this soil moisture augmentation serves as a surrogate for this process.

While it is well known that rooting zone depth is a significant determinant of available soil water, it is difficult to estimate at landscape levels. Therefore, the spatial patterns of rooting zone depth represents a potentially important source of model uncertainty.

Carbon–nitrogen allocation model

In order to grow LAI dynamically a carbon (C) and nitrogen (N) allocation model modified from Running and Gower (1991) was added to RHESys. The allocation model annually allocates photosynthate and available N to leaf, stem and root components within each wetness interval. Annual allocation of C to the canopy (foliar, root and stem) is determined by three limitations:

$$C_{LC} = PSNR_{L/R} \quad (\text{photosynthate limitation}) \quad (6a)$$

$$C_{LP} = C'_L \frac{\Psi_{SC}}{\Psi_{\max}} \quad (\text{water limitation}) \quad (6b)$$

$$C_{LN} = \frac{N_{\text{Avail}} R_{L/R}}{N_{\text{leaf}}} \quad (\text{nitrogen limitation}) \quad (6c)$$

where $R_{L/R}$ is a leaf–root partitioning ratio determined by soil moisture and available nitrogen (N_{Avail}), PSN is annual net photosynthesis (kgC ha^{-1}) computed by the daily gross photosynthesis model of Lohammar *et al.* (1980) minus respiration losses, C'_L (kgC ha^{-1}) is current-year leaf carbon, Ψ_{max} (MPa) is the maximum leaf water potential reached during the growing season, and N_{leaf} (kgN kgC^{-1}) is the leaf nitrogen concentration. The most limiting of Equations (6a)–(6c) determines the actual percentage of assimilated carbon that is allocated to the leaves: $C_L = \min(C_{LC}, C_{L\Psi}, C_{LN})$. The leaf–root ratio then determines allocation of the remaining photosynthate to the roots and stem (bole and branches).

The value of N_{Avail} (kgN ha^{-1}) is computed using a decomposition model having litter and mineral soil compartments. A non-linear function of soil moisture was parameterized to obtain optimal decomposition rates at soil moisture conditions less than saturation, and rapid reduction of decomposition rates in water-logged soils. Decomposition is computed daily to respond to soil moisture and temperature dynamics, but integrated to annual values for use in the allocation equations. Finally, N loss is computed using a non-linear function of the total available N, following the approach used in BIOME–BGC (Running and Hunt, 1993).

Carbon and nitrogen pools are maintained in the mineral soil, litter, roots, stems and leaves within each wetness interval on each hillslope. C_L is used to compute the LAI as

$$\Lambda_T = \Lambda_{\text{Sp}} C_L \quad (7)$$

where Λ_{Sp} ($\text{m}^2 \text{kgC}^{-1}$) is a species-specific leaf area. Annual C and N contributions from the canopy to the litter are relatively small compared with the total litter and soil pools. Thus, year to year interaction of LAI is minimal. However, the soil and litter pools are difficult to initialize spatially, so these pools tend to adjust over time to reflect spatial patterns of vegetation, soil moisture and temperature. Long-term adjustment of these large pools will influence the trend in LAI.

Within each elevation band, the canopy model is executed over the joint distribution of wetness intervals, vegetation and soil parameters. In the current model structure, bulk water transfers into and out of the saturation zone (e.g. recharge, baseflow, saturation deficit redistribution) are executed at the hillslope level. The entire watershed is then represented by the spatial distribution of hillslopes. Since elevation bands introduce the potential for variable timing of snowmelt along a hillslope, it is possible for this model structure to introduce spatially variable vertical recharge to the saturated zone. In this way, the model structure may have a direct influence on the timing of the snowmelt hydrograph. If water transfers from each elevation band can be shown to occur largely through channelization it may be reasonable to modify the model to account for bulk water transfers at the elevation band level. Otherwise, an alternative solution to variable recharge would have to be considered.

METHODOLOGY

Study sites

Onion Creek is a 13 km^2 watershed located in the Central Sierra Nevada in California. Relief in this watershed is about 1000 m with the highest elevation at about 2600 m a.s.l. Annual precipitation of about 1300 mm occurs predominantly as snowfall, and snowmelt is the main source of soil water for the old-growth mixed coniferous vegetation. From the end of snowmelt, in early June, to early September there is a rapid drop in available soil water.

Figure 3 shows the RHESSys partitioning scheme, which breaks Onion Creek at a grid resolution of 30 m into 34 hillslope partitions, 10 elevation zones and wetness intervals (χ_i). The digital elevation model is from a mosaic of USGS 7.5' quadrangles for the Truckee, California area. Distributed LAI for Onion Creek was estimated from Landsat Thematic Mapper (TM) bands 3, 4 and 5 using methods described in Nemani *et al.* (1993).

The Turkey Lakes Watershed (TLW) (Figure 4) is a 10.5 km^2 experimental watershed located in the Algoma Highlands, 60 km north of Sault Ste Marie, Ontario, Canada. Relief within the basin is about

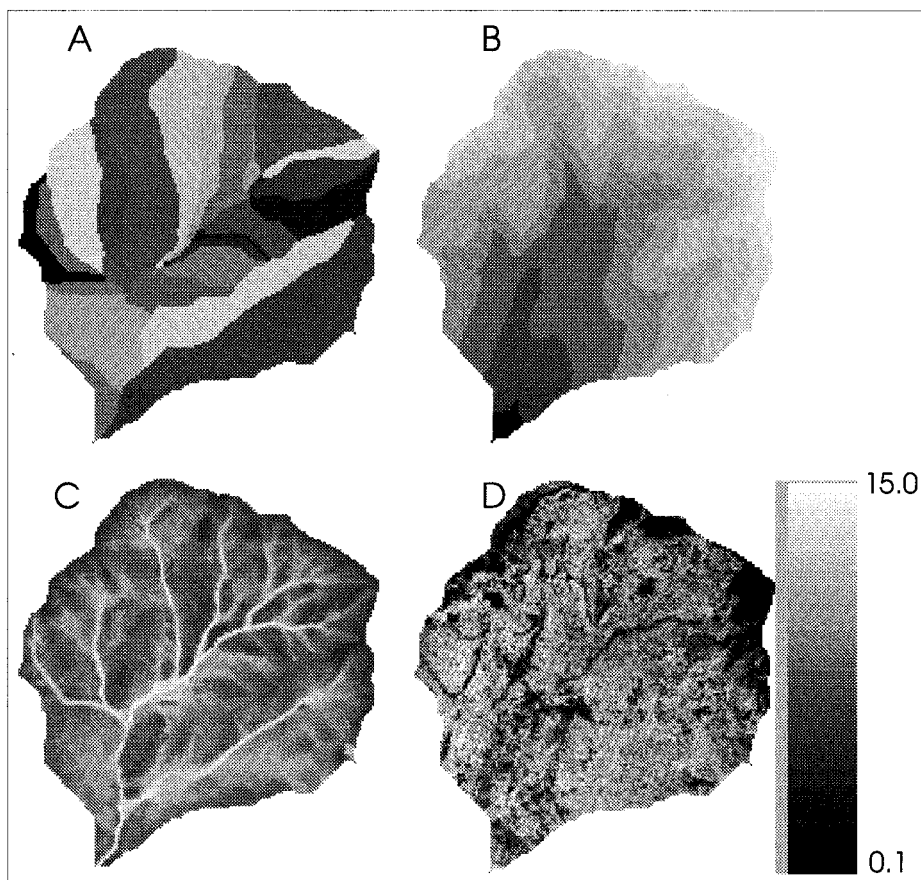


Figure 3. Spatial description for Onion Creek showing hillslope partitions (A), elevation zones (B), wetness intervals (C) and leaf area index (D)

300 m with the highest elevation at 630 m a.s.l. Mean annual precipitation during the 1980s was about 1250 mm. Soils are well-developed Orthic Hummo-feric Podzols on silty to sandy-textured till, which overlies a Precambrian bedrock of mafic to intermediate metavolcanics. The area is transitional between the Great Lakes–St Lawrence lowland forest region and the boreal forest region to the north, with boreal herbs occurring on northern exposures and cold drainage sites. Sugar maple (*Acer saccharum* Marsh.) and yellow birch (*Betula lutea* Michx. f.) dominate drier upland sites, while tamarack (*Larix laricina* [DuRoi] K. Koch.), black ash (*Fraxinus nigra* Marsh.) and sugar maple dominate wetter sites of highly humified organic deposits, which occur in bedrock-controlled depressions and areas adjacent to streams and lakes (Jeffries *et al.*, 1988). About 15% of the TLW is lake or wetland. Following Mackay and Band (1994) the full TLW watershed, including lakes, may be extracted and represented as in Figure 5. Partitioning is derived from a 5 m resolution digital elevation model, which was interpolated from a digitized contours map. Catchment TLW-C34 is the largest, with the most relief in the area, of all TLW catchments. Figure 6 shows the breakdown of TLW-C34 into 22 hillslope partitions, three elevation zones and wetness intervals at 0.5 increments. Distributed LAI for TLW-C34 was obtained from TM bands 3 and 4. This LAI image is intended to represent spatial patterns of relative canopy depth, rather than absolute values of leaf biomass. As the TLW has a deciduous forest cover, leaf phenology is simulated using a simple linear leaf-out period from a fixed leaf-on date. Leaf-out is assumed to take one week. In the autumn, LAI ramps down linearly over a period of three weeks to a fixed leaf-off date. TLW-C34 and Onion Creek are undisturbed

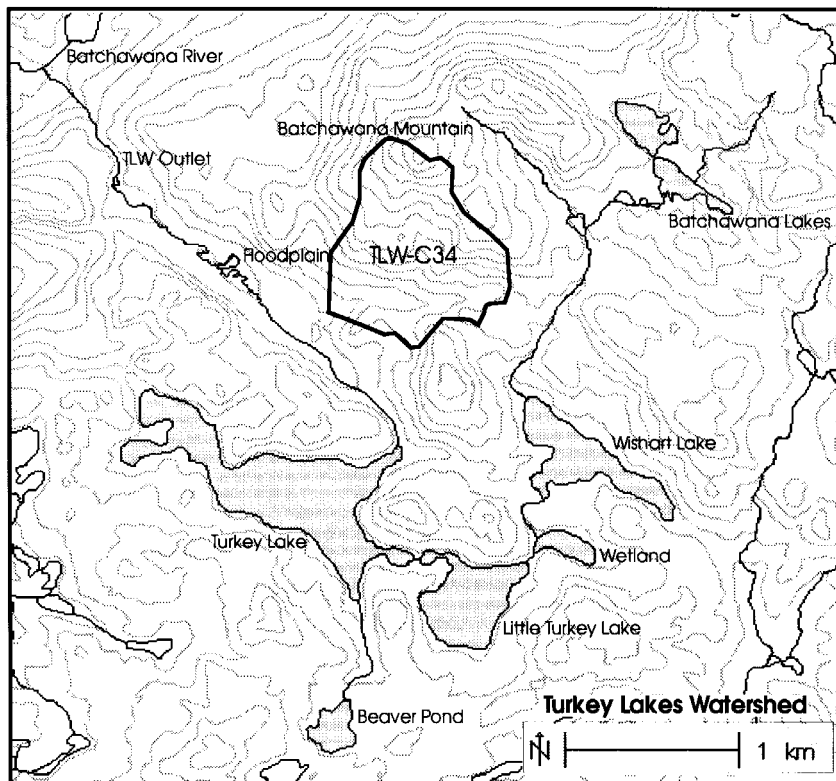


Figure 4. Map of the Turkey Lakes Watershed showing its main features, including catchment C34

catchments. In these simulations we assume that a single life form (conifer or deciduous) dominates each watershed.

Figure 7 shows the covariation of LAI with wetness intervals for both Onion Creek TLW-C34. The Onion Creek LAI–wetness index covariation is characteristic of a water-limited environment, with a generally asymptotic LAI in moderate to high wetness areas. LAI in TLW-C34 shows a negative relationship with wetness. The LAI is relatively uniform across the dry to moderately wet sites, but declines towards the wetter sites. Although the TLW receives only about 25% more precipitation than Onion Creek, precipitation is relatively uniformly distributed throughout the year, whereas Onion Creek receives most (about 80%) of its precipitation as snow. In the TLW evaporative demand may not exceed precipitation recharge of the soil, owing to the frequency with which summer rainfall occurs. Evaporative demand on Onion Creek is relatively high compared with available soil moisture.

Experimental design

Prescribed canopy. The goal of this experiment is to determine if hydrological outputs from a watershed are sensitive to the spatial covariance of vegetation, topographic position (χ) and soil (i.e. the catenary sequences characteristic of the landscape). A null hypothesis can be formulated that states that runoff production does not differ between a simulation incorporating the spatial patterns of vegetation on the terrain compared with a simulation that does not incorporate vegetation patterns. This hypothesis is tested by examining the change in outflow between simulations run with a watershed average LAI and with a spatially distributed LAI, which is obtained from remotely sensed imagery. Watershed LAI and distributed LAI thus yield the same watershed total leaf biomass. Note that the canopy carbon allocation and growth modules are not used in

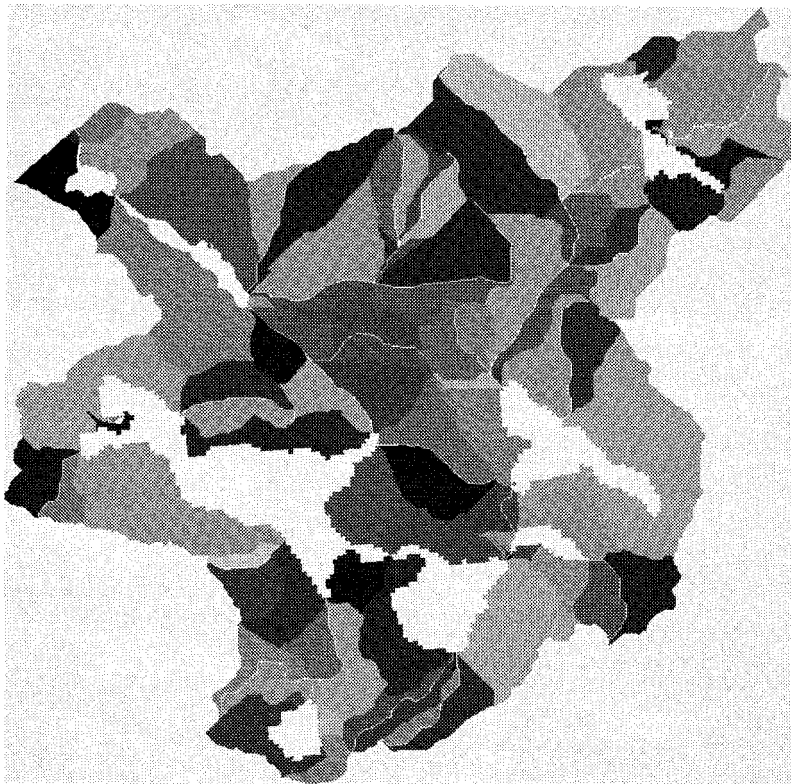


Figure 5. Full partitioning of the TLW including hillslopes, streams and lakes

these simulations. LAI is not computed with Equation (7) in this simulation but is set as a spatial pattern at the wetness interval level for a one-year simulation.

In order to account for the effect of rooting depth on the sensitivity of outflow and evapotranspiration to distributed versus stand LAI, both 70 cm (shallow) and 140 cm (deep) rooting zone depths are prescribed in parallel experiments. Four simulations are made using prescribed LAI for both study sites. The simulations are: (1) uniform (or watershed expected) LAI with a shallow rooting depth; (2) distributed LAI with a shallow rooting zone; (3) uniform LAI with a deep rooting zone; and (4) distributed LAI with a deep rooting zone.

Dynamic canopy. The previous section addresses the question of whether hydrological outputs are predictable from vegetation controls on the distribution of net water sources. Here we address how sensitive distributed watershed water and carbon budgets are to rooting depth. The hypothesis is that the vegetation carbon and water flux processes are less sensitive to hydrological flow paths, or water availability extremes, as rooting depths increase. A larger rooting depth suppresses the variation in vegetation growth and evapotranspiration between wet and dry sites. To examine this hypothesis the dynamic allocation model is incorporated in order to allow the LAI to develop with respect to the spatial distribution of soil moisture and nutrients, and to temporal changes in climate forcing.

For the purposes of this experiment an even-aged forest is assumed in order to initialize the model with leaf/stem and leaf/root ratios based only on a knowledge of LAI. Stem C is assumed to be 30 times that of the canopy, and root C is assigned to be 4.5 times the canopy C. Leaf C is computed by rearranging Equation (7). Soil and litter C and N pools are initialized using values reported in Mitchell *et al.* (1992) and Morrison

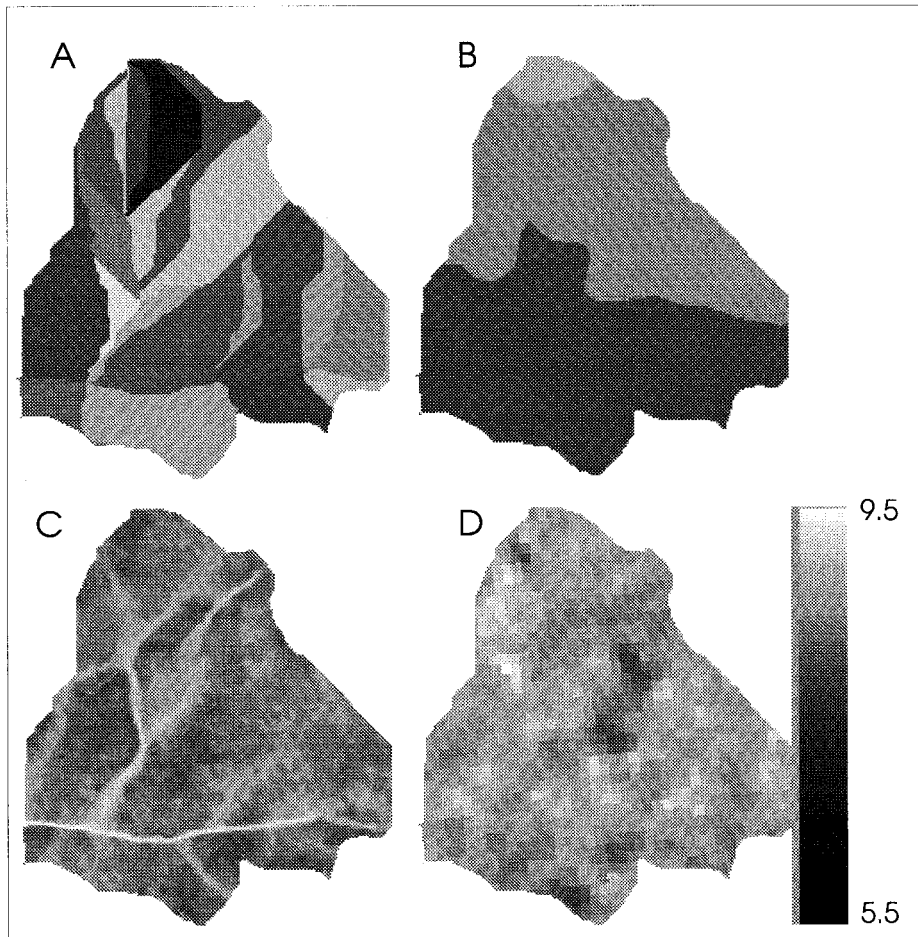


Figure 6. Spatial description for TLW-C34 showing hillslope partitions (A), elevation zones (B), wetness intervals (C) and leaf area index (D)

(1990) for other sites within the TLW. Two simulations are made: (1) a 100-year simulation with a 70 cm rooting depth; and (2) a 100-year simulation with a 140 cm rooting depth. A 100-year climate record is generated by replicating a 10-year meteorological record over 10 cycles. This allows for comparisons to be made at two spatial scales: watershed average responses and spatial variation of responses, and two temporal scales: year to year fluctuations and long-term trends. Long-term trends reflect the effects of the model initialization of the slowly varying stores in the model (canopy biomass, and soil and litter carbon and nitrogen pools), rather than interannual weather variations. The 100-year simulation period should indicate differences in the temporal length scales at which different variables are operating. For instance, it is expected that soil N varies over a longer period of time than available N, since it represents a large pool relative to the annual N turnover from the leaves.

RESULTS

Prescribed canopy in Onion Creek

Figure 8a shows the simulated discharge hydrograph for Onion Creek using a spatially uniform LAI with a uniform 70 cm rooting depth for the period beginning with the start of snowmelt to the end of the year.

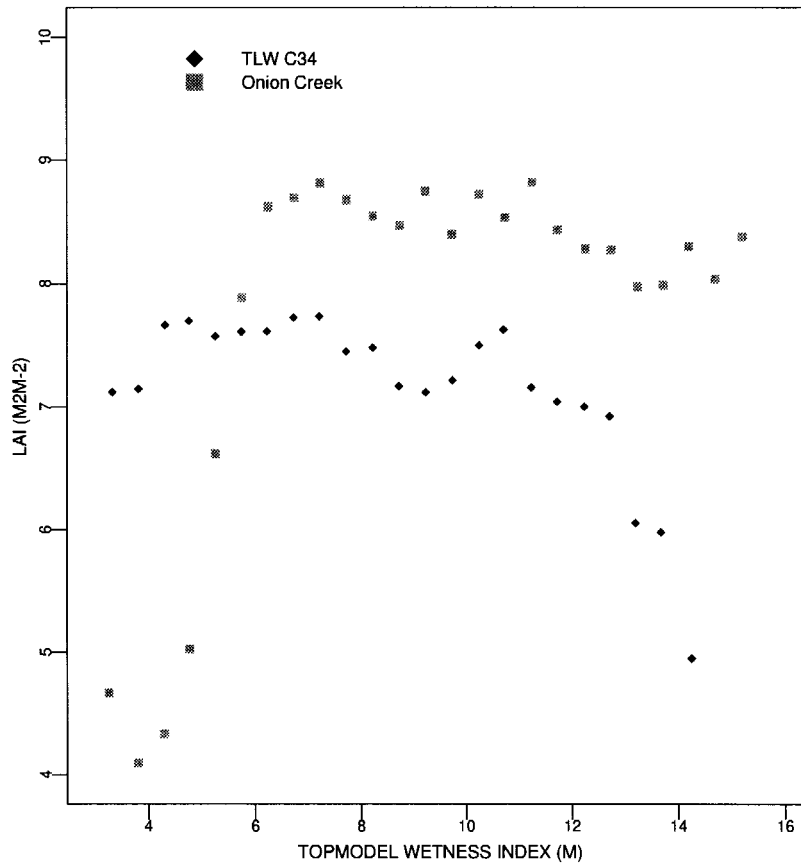


Figure 7. Relationships between LAI and wetness index for Onion Creek and TLW-C34. The positive relationship for Onion Creek indicates that this site is water limited. TLW-C34 shows a negative relationship, which suggests that some sites may have too much water

Table I summarizes the annual totals of the hydrological outputs, controls on the outputs and net photosynthesis for each of the four simulations. In this table, direct precipitation refers to precipitation and snowmelt on saturated surfaces. In Onion Creek, most of the annual precipitation is stored in the snowpack and is released in a short time period, yielding relatively high values for the proportion of precipitation following this pathway. It is interesting that direct precipitation runoff from saturated areas is the most sensitive to a change from stand to distributed vegetation. This is attributable to a predominance of runoff production during the snowmelt period when saturated areas cover a relatively large area. Since these saturated areas correspond to high LAI sites they represent the areas most sensitive to variability in direct runoff.

Table I. Onion Creek diagnostic variables. Water balance variables are shown as a percentage of precipitation

	Direct precipitation (%)	Return flow (%)	Baseflow (%)	E (%)	T (%)	ΔS (%)	PSN (gC m^{-2})
U70	31.16	2.45	13.03	13.31	31.50	6.56	1183.79
U140	29.46	2.21	12.26	15.31	33.61	7.15	1246.44
D70	21.62	8.71	15.95	15.64	31.66	6.42	1092.73
D140	18.85	7.27	14.47	15.64	36.99	6.78	1234.32

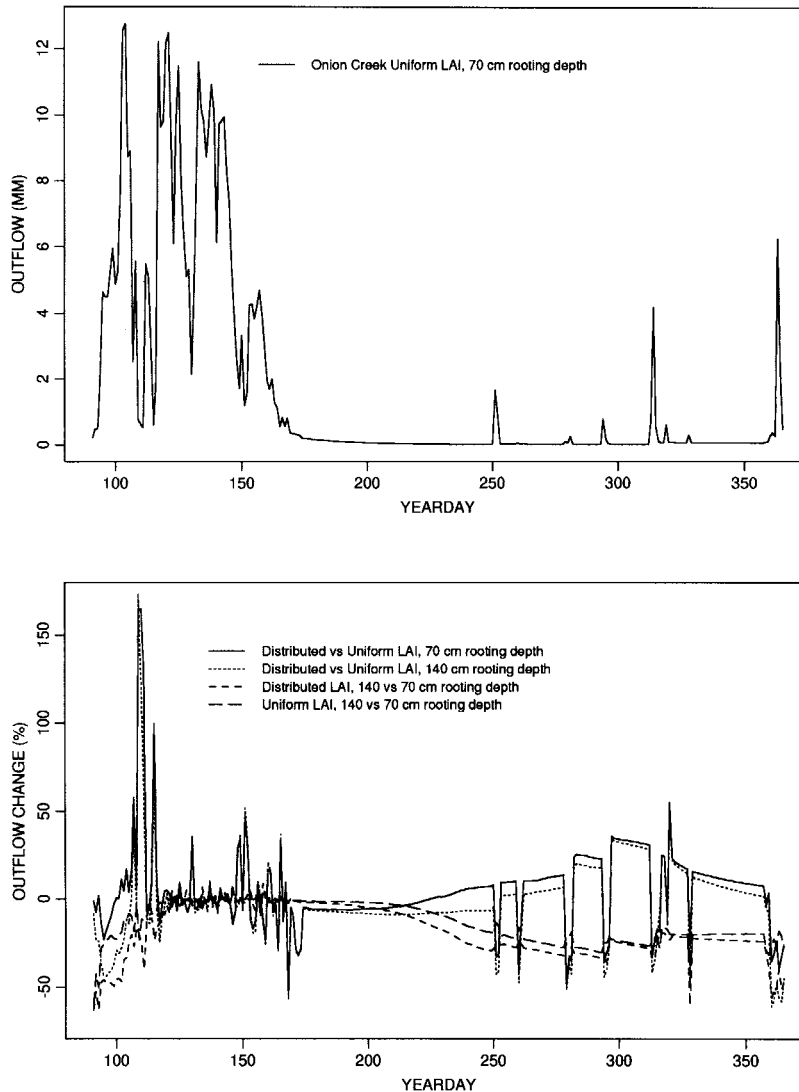


Figure 8. Graph (a) shows the discharge hydrograph for Onion Creek for the period beginning just before snowmelt and ending at year-end. The graphs in (b) show comparisons made between distributed vs. stand LAI, with both shallow and deep rooting zones

Simulations are first spun up with one year of meteorological data to initialize state variables, then repeated with the same meteorological input. Note that the conditions of snowpack and saturation deficit at the beginning of the year reflect those of the end of the same year. Figure 8b shows the percentage change in outflow with a distributed LAI rather than a uniform LAI, for both the 70 cm and 140 cm rooting depth. Also shown are the effects of changing rooting depth without changing LAI. The snowmelt period is characterized by changes to the timing of snowmelt from different parts of the watershed. The early snowmelt hydrograph, which is contributed from high LAI sites near the streams, is delayed owing to increased radiation interception by the higher LAI canopy on the wetter sites. This allows for snowmelt contribution from higher and lower elevation sites to occur simultaneously, resulting in increased return flow. During snowmelt the effect of rooting depth is negligible, as there is very little transpiration at this time.

Distributing the LAI has the effect of increasing summer low flows. Using an average LAI uniformly distributed over the watershed areas, sites near the streams and ridges receive the same total LAI of 8. Using the distribution shown in Figure 7, sites in the valley bottoms are assigned LAI values in excess of 8, while the drier ridge sites receive lower LAI. The gradual positive increase in the change in low flow with this distribution of LAI is a result of the change in the distribution of evapotranspiration. The areas around the stream transpire a greater amount, resulting in an overall localized increase in annual total evapotranspiration. The increase in transpiration in these sites is not proportional to the increase in LAI, owing to the asymptotic relationship between LAI and absorbed radiation. In contrast, the drier sites, with lower LAI, transpire at a reduced rate that is more linearly related to the decrease in LAI. Low LAI sites correspond to higher elevation sites in steep catchments. Thus, higher elevation sites, which receive greater precipitation and lose their snowpack later in the spring, contribute a greater recharge to the saturated area with a reduced LAI and transpiration demand. This results in an annual total baseflow increase of about 30 mm. Note that late summer and autumn runoff events are noticeably reduced with a distributed LAI, since precipitation over areas of surface saturation is intercepted and evaporated directly as a result of higher LAI. It should be noted that lower LAI in high elevation sites also promotes earlier radiation-driven snowmelt in these areas, which would tend to increase early summer evapotranspiration rates in these areas and potentially reduce summer low flows. The influence of model structure may be evident here. For instance, if flow from elevation zones were predominantly channelized, then elevation zone saturation deficits may be more localized properties during snowmelt. As such, the distributed and stand LAI on summer low flows may be slightly exaggerated in the simulations.

The effect of having a deep rooting zone is to increase total transpiration and reduce the net source of water to subsurface flow paths. This effect is greater with distributed LAI than with watershed average LAI, and is the result of a delay in the reduction of soil moisture levels to wilting point over a larger fraction of the watershed. Areas with a moderately high LAI are able to transpire at higher rates further into the summer, whereas with watershed average LAI the rates of transpiration are reduced in these areas. This argument is supported by the observation that on day 300 the distributed and stand LAI curves showing differences between deep and shallow rooting have converged. Thus the distribution of vegetation has regular influences on the partitioning and timing of hydrological outputs. Although the magnitude of the changes caused by vegetation are small compared with the typical differences between simulated and observed outflows, the changes lead to a directional bias and appear to be more significant under conditions of shallow rooting depth. The lack of unsaturated soil water recharge via capillarity in the model may partially account for differences attributed to shallow and deep rooting zones, but capillarity cannot fully compensate for a deep root system.

These observations are summarized as follows.

- (1) Well-drained, high elevation sites that are connected contribute significantly to summer baseflow. Watershed average values for LAI result in significantly underestimated low flows.
- (2) High LAI values over partial contributing areas intercept significant amounts of summer and autumn precipitation. Watershed average LAI results in an overestimation of summer peak flows.
- (3) High LAI in wetter sites that correspond with lower elevation sites delays the early snowmelt runoff. In addition, early snowmelt is contributed by a larger portion of the watershed, as melting in areas with lower LAI is accelerated.
- (4) Greater rooting depth increases transpiration rates and reduces the magnitude of the hydrological response to distributed canopy cover by increasing and homogenizing available water supply.

Prescribed canopy in TLW-C34

Figure 9a shows the simulated and observed discharge hydrographs for TLW-C34 for the year 1987, which was the driest (1087 mm of precipitation at the base station) year of the meteorological record, and year 1988, which was the wettest (1550 mm at the base station) year on record, using stand LAI and the shallow

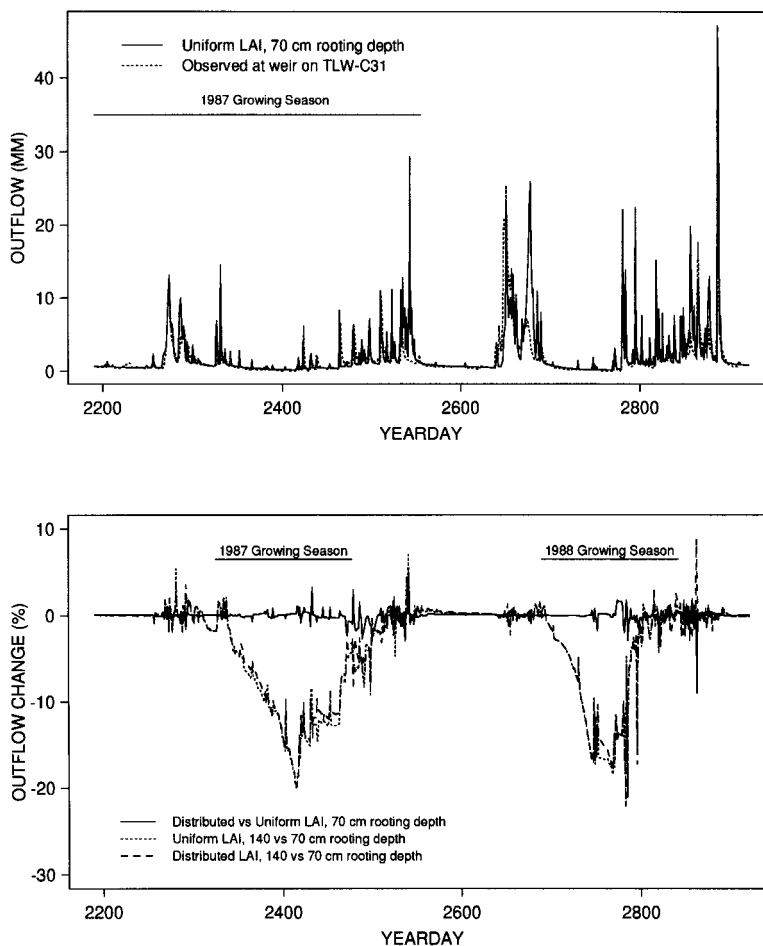


Figure 9. Graph (a) shows the discharge hydrograph for TLW-C34, as well as the discharge observed at the weir. Years 1987 and 1988 are shown, as they are representative of dry and wet years, respectively, in this area. The graphs in (b) show comparisons made between distributed vs. stand LAI, and shallow and deep rooting zones

rooting depth. Table II summarizes the annual totals of the hydrological outputs, controls on the outputs and net photosynthesis for the TLW-C34 simulations. In contrast to the snowmelt-dominated Onion Creek, this watershed exhibits major rainfall–runoff events from about midsummer to mid-spring. Overall, the model captures the response of TLW-C34, with a few notable exceptions. First, the model overestimates discharge events at the end of the snowmelt periods in both years. This excess simulated discharge not observed at the weir implies that either, (1) precipitation in TLW-C34 differs from the precipitation observed at the meteorological station, which is about 2 km away on the other side of Batchawana Mountain; (2) there is some macropore flow that RHESSys is currently not accounting for; or (3) the snowmelt model, which was designed for dry mountainous environments, is a poor representation of snowmelt in cool, humid environments. In addition, RHESSys assigns daily precipitation as either snow or rain as a function of daily average temperature. Precipitation that fell as rain when daytime temperatures were just above freezing and nighttime temperatures were below freezing may fall as snow in RHESSys simulations. Precipitation partitioning requires subdaily resolution meteorological data, which is seldom available in long-term records.

Figure 9b shows a comparison between distributed and stand LAI for both shallow and deep rooting depths. The effect of distributing LAI is negligible, as the distribution of LAI in the TLW does not show the

Table II. TLW-C34 diagnostic variables. Water balance variables are shown as a percentage of precipitation

	Direct precipitation (%)	Return flow (%)	Baseflow (%)	E (%)	T (%)	ΔS (%)	PSN (gC m ⁻²)
1987							
U70	21.52	1.23	36.70	28.38	19.97	-7.80	571.95
U140	21.14	1.19	35.89	28.38	21.18	-7.78	602.24
D70	21.52	1.21	36.68	28.38	20.01	-7.79	572.00
D140	21.08	1.21	35.89	28.38	21.22	-7.78	602.11
1988							
U70	26.50	4.71	36.02	15.09	13.66	4.03	611.47
U140	26.18	4.70	35.57	15.09	14.45	4.02	646.11
D70	26.48	4.75	35.97	15.08	13.69	4.02	610.84
D140	26.18	4.71	35.54	15.08	14.47	4.02	645.18

extremes exhibited in Onion Creek. In the TLW the higher LAIs are distributed on to areas closer to the ridges (see Figure 7), and the growing season is characterized by frequent small precipitation events that recharge the soil. With a deeper rooting zone there is a drop in growing season outflow corresponding to higher transpiration rates. The magnitudes of the changes to stream flow discharge, as a result of increased transpiration, are similar between the relatively dry and wet years. However, this effect occurs over a shorter time in the wet year (1988) as a result of large rainfall events shortly after the middle of the growing season. Frequent recharge to the soil acts as a buffer against soil water losses and reduces the sensitivity of transpiration to rooting zone depth. Precipitation and depth of the rooting zone act as similar controls on available water. For two hydrologically similar locations, if we integrate soil water over the growing season, then total available water to vegetation in a semi-arid environment with deep rooting zones should be similar to total available soil water to vegetation in humid environments with shallow rooting zones.

The simulation results for the prescribed LAI in the TLW are summarized as follows.

- (1) Stream flow discharge is not sensitive to the distribution of LAI in the humid, TLW environment. This result is, in part, a result of a relatively homogeneous LAI, which really only distinguishes between upland, dense vegetation, and lowland, gapped vegetation. In addition, frequent summer precipitation reduces the relative magnitude of evaporative demand with respect to precipitation inputs.
- (2) Rooting depth has an effect on transpiration losses and its effect is most noticeable on baseflow. The effects of rooting zone are most noticeable in the semi-arid environment, and most noticeable during the driest year in the humid environment. As expected, precipitation, and in particular frequency of precipitation, and rooting zone depths result in similar vegetative response.

Sensitivity of a dynamic canopy to the coupling with hydrology

Figures 10 and 11 show LAI, stem C, available N, and soil N for 70 cm and 140 cm rooting depths, respectively. The results are for 100 years simulated with the 10 cycles of the 10-year meteorological record available. Solid lines are catchment mean values, while the dashed lines show the mean plus or minus one standard deviation. The first 10-year cycle shows initialization effects and should be ignored. This initialization effect is as a result of our uncertainty in assigning leaf/stem and leaf/roots ratios, as evidenced by the increasing allocation to stem C. In general, the variation in LAI in space remains constant between years, although the mean responds to differences in annual climate. Average LAI is higher (by about 2) and spatial variation is reduced with the deeper rooting zone, supporting the hypothesis that the depth of rooting zone determines the buffering to hydrological flow path distributions. The deeper rooting zone also results in a greater fluctuation in LAI between years. This difference is owing to the forest declining in the shallower rooting zone (Figure 12). These areas become inactive once the LAI drops too low to assimilate enough carbon to grow.

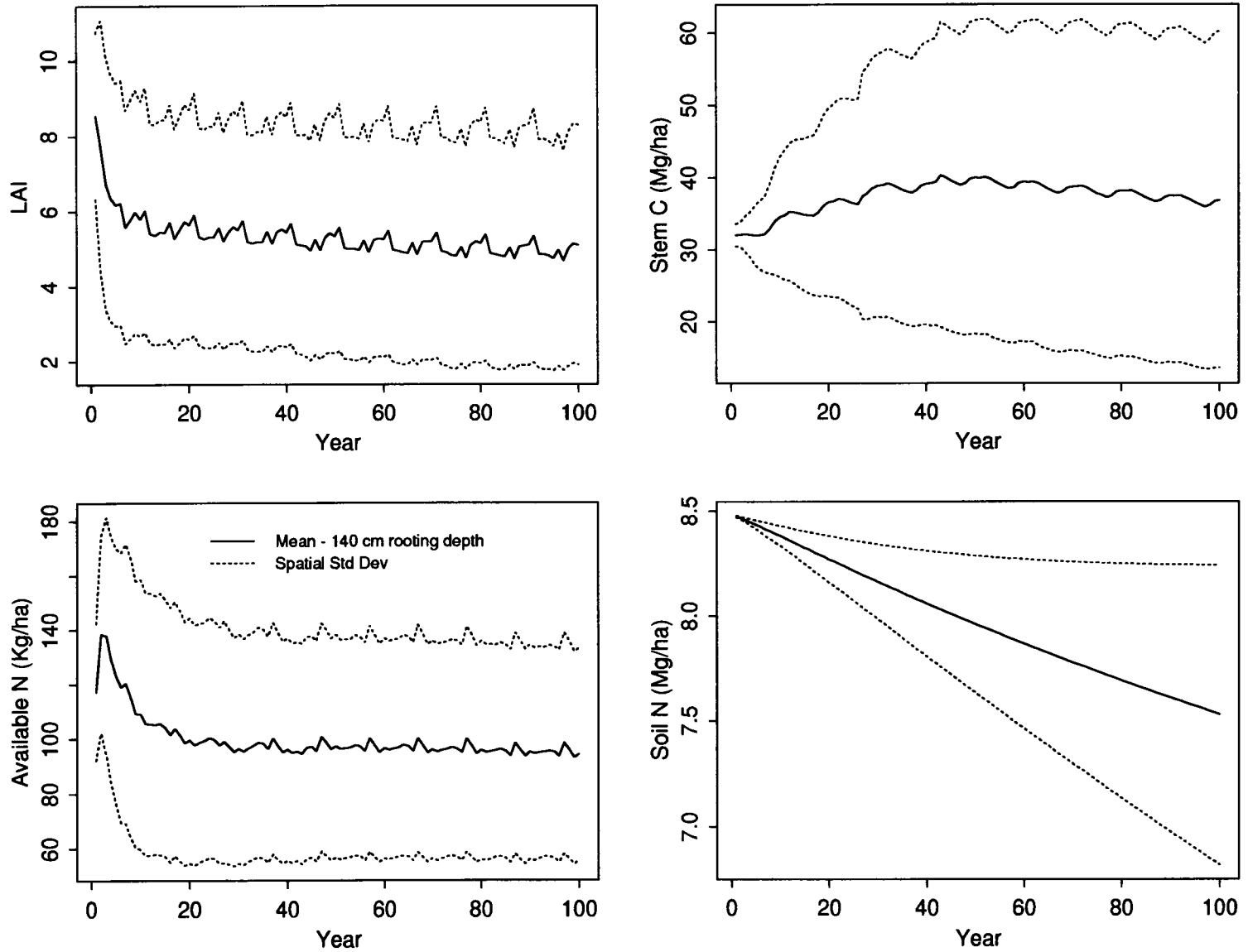


Figure 10. Shown are LAI, stem C, available N and soil N over a 100-year simulation using the dynamic canopy model with a shallow rooting zone. The solid lines represent catchment mean responses, while the dotted lines envelope the spatial standard deviation from the mean

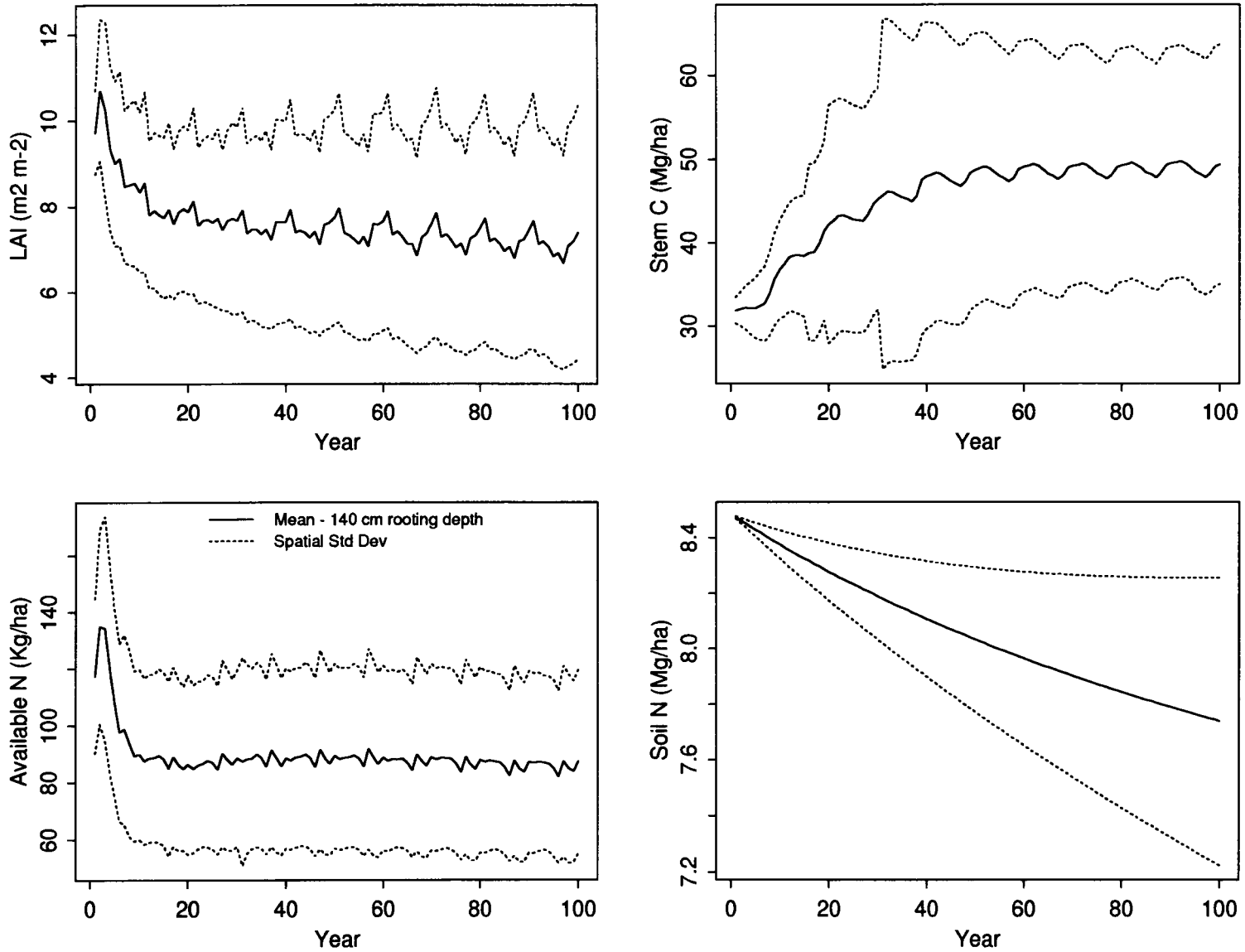


Figure 11. Shown are LAI, stem C, available N and soil N over a 100-year simulation using the dynamic canopy model with a deep rooting zone. The solid lines represent catchment mean responses, while the dotted lines envelope the spatial standard deviation from the mean

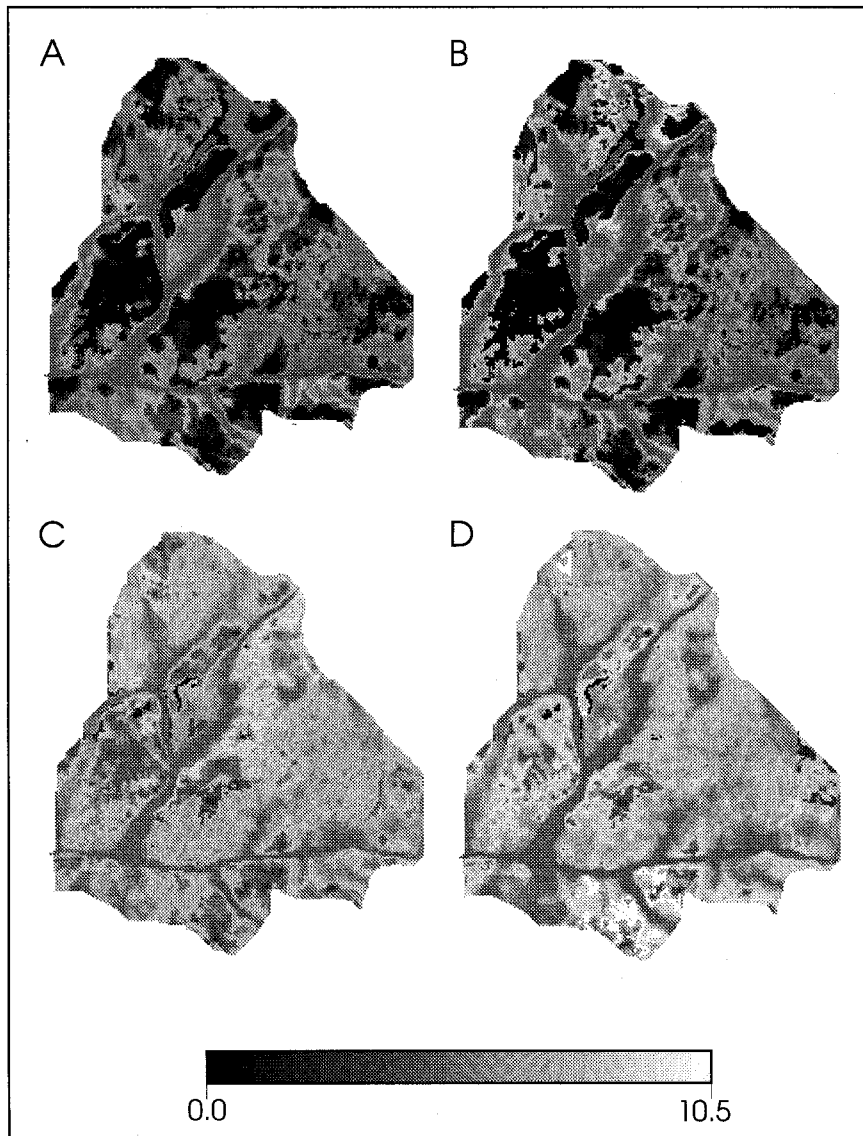


Figure 12. Spatial patterns of simulated LAI for shallow (A,B) and deep (C,D) rooting depths. Images (A) and (C) are for the dry year (1987), and images (B) and (D) are for the wet year (1988)

Figure 12 shows the spatial patterns of LAI for the dry (1987) and wet (1988) years for a second cycle of the 100-year simulations (the first 10-year cycle is a spin up period), for both shallow and deep rooting depths. With a shallow rooting depth the spatial variation in LAI is higher than expected for old growth conditions. In particular, low wetness interval sites exhibit strong water limitations resulting in significant areas with no canopy supported. This problem does not occur with the deeper rooting zone, which produces less overall spatial variation. The spatial variation in LAI with a deep rooting zone is attributed to radiation differences between hillslopes, and differences in average soil moisture. This latter contribution is highly dependent upon the topographic analysis that went into production of the TLW digital elevation model and extraction of specific catchment areas and local slopes. Areas of high wetness index inhibit C allocation to the leaves, since decomposition rates in these areas are reduced during extended periods of saturation. While the

general reduction in canopy density in the riparian areas is consistent with observation both in the field and on aerial photographs, reduction in N mineralization is not the direct cause of this canopy thinning. Foster *et al.* (1989) found that not all leached nitrate from a nearby catchment within the TLW reaches the stream. They suggested that denitrification in the riparian areas may account for this loss of nitrate. Poorly aerated soils in the saturated areas may account for reduced N uptake by the trees, and, in turn, reduced N available to the plants. Currently, the model does not simulate denitrification, reduced N uptake processes or lateral transfer of N. If reduced LAI is attributable to nutrient deficiency, then an accurate representation of the areal extent of saturated areas is needed to simulate patterns of forest growth in the TLW. These processes are explored by Creed *et al.* (in press).

In general, spatial patterns of simulated LAI remain stable between years under old growth conditions, with a few notable exceptions. Drier areas generate relatively higher leaf biomass during a wet year than a dry year. As 1987 was an exceptionally dry year, the reduced LAI is a response to lower wetness intervals showing water stress, resulting in a greater allocation to the roots and a reduced allocation to the canopy. Moderate to high wetness intervals show little response to the water stress. During the exceptionally wet year 1988 some of the higher wetness intervals show greater N limitation, as an indirect response to reduced saturation deficits.

SUMMARY AND CONCLUSIONS

There are many vegetation (e.g. maximum stomatal conductance, maximum mesophyll conductance) and soil (e.g. porosity, characteristic curve) parameters that are never without uncertainty and could have been varied in this sensitivity analysis. For instance, Kelliher *et al.* (1995) summarize life form stomatal conductance rates measured by different researchers and show that there is greater variation between studies than between life form. In this study we used canopy average stomatal conductance rates reported in Running and Hunt (1993). However, vegetation coverage is also subject to short-term change as a result of disturbance. The distribution of vegetation is tightly coupled with the distribution of soil water, having developed in response to available soil water within climatic constraints. The first question asked was if simulated bulk hydrological outputs from a watershed showed predictable responses to the spatial distribution of vegetation. To answer this question a comparison was made between hydrological outputs under a stand average LAI for the watershed versus outputs under a fully distributed LAI. In Onion Creek, vegetation patterns influence snowmelt timing as a result of changes to intercepted radiation. During the summer months relatively high LAI in the valley bottoms and low LAI in the drier sites generates, overall greater subsurface flow owing to a net reduction in transpiration and greater overall contribution of these better drained sites as sources for throughflow recharge. This pattern is predictable, since evaporative demand greatly exceeds precipitation during the summer months. The higher LAI in the partial contributing areas resulted in a decrease in summer direct precipitation runoff owing to increased interception losses. The high LAI sites also had asymptotic transpiration responses to increased LAI, while the low LAI sites had a more linear response to a reduction in LAI. These patterns were not detectable in TLW-C34, since the spatial variation in LAI in this catchment was significantly less than that of Onion Creek, and frequent summer precipitation reduced relative evaporative demand in comparison with available soil water.

It was argued that limiting available soil water, which is determined in RHESSys in part through precipitation, soil hydraulic properties and rooting zone depth, would determine the covariation of vegetation with hydrological flow paths. In Onion Creek a greater rooting depth results in greater transpiration losses, which partially offsets the reduction in transpiration with distributed LAI. As rooting depth is increased to the extent that water limitations are eliminated then evapotranspiration would reach potential rates, which should support higher productivity and high LAI regardless of the flow paths. If water is non-limiting then the distribution of LAI in Onion Creek would also show negligible control on subsurface flow as observed in the TLW. The purpose of incorporating TOPMODEL into RHESSys was to obtain a realistic spatial pattern of soil moisture that determine evapotranspiration and PSN rates (Band *et al.*, 1993). It seems that a good method of obtaining appropriate spatial distributions of rooting depth, along with soil

hydraulic properties, is essential for accurate simulations of spatial patterns of vegetative recovery. The equilibrium response of vegetation in water-limited environments is a direct response of soil hydraulic properties (Nemani and Running, 1989) and landscape position. Carbon allocation to the canopy is sensitive to rooting depth. Since changing rooting depth is a substitute for changing soil hydraulic properties, even environments with frequent precipitation, such as the TLW, cannot be accurately portrayed without a knowledge of the effective soil hydraulic properties of the rooting zone. We recognize that capillarity may significantly reduce the sensitivity of the vegetation to rooting zone depth, since it would recharge the available soil water even as the water table drops below the rooting zone.

We conclude with suggestions of how to pursue the problems identified in this paper.

- (1) Specific life form distribution within undisturbed watersheds may reflect adaptation to some adjusted, catenary condition. Band *et al.* (1993) chose to define rooting depth as the full soil depth, as they were working in mountainous catchment with thin soils. However, rooting depths may reflect species adaptation to maximize water use in order to avoid water stress. With all soil hydraulic properties held constant, rooting depth at a particular location may be more related to the long-term average local saturation deficits, rather than the depth of the full soil profile. Sala *et al.* (1996) have recently proposed a simple rooting depth model for vegetation that increases local rooting depth to the point that no further increases of transpiration occur. This has been applied to plot studies in arid to semi-arid zones where water limitation is the primary limiting factor. Modification and application to a wider range of environments and to distributed models may be a promising approach.
- (2) The upper tail of the distribution of wetness index should be accurately represented in order to capture the riparian dynamics, particularly in more humid sites. Although the position of wetness intervals with respect to the mean wetness of a hillslope determines relative wetness and total runoff production, the shape of the upper tail determines the extent of saturated areas that persist into the growing season. With a prescribed LAI and leaf N content it was not critical to model the riparian dynamics. By explicitly simulating soil decomposition and carbon allocation processes we are forced to consider the significance of the upper tail of the wetness index distribution.
- (3) The importance of model structure on the interpretation of the results has been addressed in a few places in this paper. One issue raised is that spatial variability of vertical recharge to the saturated zone results from interactions between the saturated soil layer and a number of components of the integrated model, such as snowmelt and spatially variable vegetation. Since the TOPMODEL wetness index assumes a spatially uniform recharge rate, spatial variability of vertical recharge is a potential source of uncertainty in the model results. For example, early spring snowmelt occurs primarily in low elevation bands. Using a hillslope scale mean saturation deficit may underestimate runoff generation and overestimate storage, thus delaying the timing and magnitude of snowmelt hydrographs. We have suggested that elevation band scale mean saturation deficits may serve as better surrogates for scaling local deficits within elevation bands, with the provision that elevation bands exhibit near-independence in terms of connectivity of flows. We argue that similar scaling issues may occur with distributed vegetation. At present, we are working on incorporating adaptive scaling intelligence into our models to allow for spatial and temporal variability of vertical recharge, without having to abandon the TOPMODEL approach in favour of a more data intensive, explicit routing model.

ACKNOWLEDGEMENTS

This research was partially supported by a Tri-Council Greenplan EcoResearch Doctoral Fellowship (to D.S.M.), as well as by funding from NASA, NSERC and the Ontario Ministry of Natural Resources (to L.E.B.). Data for the Turkey Lakes Watershed were generously provided by Forestry Canada and Environment Canada, while data for Onion Creek were provided by the US Forest Service. Comments by two anonymous reviewers are gratefully acknowledged.

REFERENCES

- Band, L. E. 1989. 'A terrain-based watershed information system', *Hydrol. Process.*, **3**, 151–162.
- Band, L. E. 1993. 'A pilot landscape ecological model for forests in Central Ontario', *Report No. 7*, Forest Landscape Ecology Program, Forest Fragmentation and Biodiversity Project. Ontario Forest Research Institute, Ontario Ministry of Natural Resources.
- Band, L. E., Peterson, D. L., Running, S. W., Coughlan, J., Lammers, R., Dungan, J., and Nemani, R. 1991. 'Forest ecosystem processes at the watershed scale: basis for distributed simulation', *Ecol. Model.*, **56**, 171–196.
- Band, L. E., Patterson, P., Nemani, R., and Running, S. W. 1993. 'Forest ecosystem processes at the watershed scale: incorporating hillslope hydrology', *Agric. For. Meteorol.*, **63**, 93–126.
- Beven, K. 1986. 'Runoff production and flood frequency in catchments of order n: an alternative approach', in Gupta, V. K. (Ed.), *Scale Problems in Hydrology*. D. Reidel Publishing Company, Hingham. pp. 107–131.
- Beven, K. J. and Kirkby, M. J. 1979. 'A physically based, variable contributing area model of basin hydrology', *Hydrol. Sci. Bull.*, **24**, 43–69.
- Creed, I. F., Band, L. E., Foster, N. W., Morrison, I. K., Nicolson, J. A., Semkin, R. S., and Jefferies, D. S. 'Regulation of nitrate-N release from temperature forests: a test of the N flushing hypothesis', *Wat. Resour. Res.* in press.
- Foster, N. W., Nicolson, J. A., and Hazlett, P. W. 1989. 'Temporal variation in nitrate and nutrient cations in drainage waters from a deciduous forest', *J. Environ. Qual.*, **18**, 238–244.
- Freeman, G. T. 1991. 'Calculating catchment area with divergent flow based on a regular grid', *Comput. Geosci.*, **17**(3), 413–422.
- Jeffries, D. S., Kelso, J. R. M., and Morrison, I. K. 1988. 'Physical, chemical, and biological characteristics of the Turkey Lakes Watershed, central Ontario, Canada', *Can. J. Fish. Aquat. Sci.*, **45**(Suppl. 1), 3–13.
- Kelliher, F. M., Leuning, R., Raupach, M. R., and Schulze, E.-D. 1995. 'Maximum conductances for evaporation from global vegetation types', *Agric. For. Meteorol.*, **73**, 1–16.
- Larcher, W. 1995. *Physiological Plant Ecology*, 3rd edn. Springer-Verlag, Berlin.
- Linacre, E. 1992. *Climate Data and Resources: A Reference and Guide*. Routledge, London.
- Lohammar, T., Larsson, S., Linder, S., and Falk, S. 1980. 'FAST — simulation models of gaseous exchange in Scots pine', *Ecol. Bull.*, **32**, 505–523.
- Mackay, D. S. and Band, L. E. 1994. 'Extraction and representation of watershed structure including lakes and wetlands from digital terrain and remote sensing information', *Paper at Spring Meeting of the American Geophysical Union, May 1994, Baltimore*.
- Mitchell, M. J., Foster, N. W., Shepard, J. P., and Morrison, I. K. 1992. 'Nutrient cycling in Huntington Forest and Turkey Lakes deciduous stands: nitrogen and sulphur', *Can. J. For. Res.*, **22**, 457–464.
- Monteith, J. L. 1965. 'Evaporation and environment', in *Proceedings, 19th Symposium of the Society for Experimental Biology*. Cambridge University Press, New York. pp. 205–233.
- Morrison, I. K. 1990. 'Organic matter and mineral distribution of an old-growth *Acer saccharum* forest near the northern limit of its range', *Can. J. For. Res.*, **20**, 1332–1342.
- Nemani, R. R. and Running, S. W. 1989. 'Testing a theoretical climate–soil–leaf area hydrologic equilibrium of forests using satellite data and ecosystem simulation', *Agric. For. Meteorol.*, **44**, 245–260.
- Nemani, R., Running, S. W., Band, L. E., and Peterson, D. L. 1993. 'Forest ecosystem processes at the watershed scale: sensitivity to remotely-sensed leaf area index measurements', *Int. J. Remote Sens.*, **14**, 2519–2534.
- Quinn, P., Beven, K., Chevalier, P., and Planchon, O. 1991. 'The prediction of hillslope flow paths for distributed hydrological modelling using digital terrain models', *Hydrol. process.*, **5**, 59–79.
- Quinn, P., Beven, K., and Culf, A. 1995. 'The introduction of macroscale hydrological complexity into land surface–atmosphere models and the effect on planetary boundary layer development', *J. Hydrol.*, **166**, 421–444.
- Running, S. W. and Coughlan, J. C. 1988. 'A general model of forest ecosystem processes for regional applications. I. Hydrologic balance, carbon gas exchange and primary production processes', *Ecol. Model.*, **42**, 125–154.
- Running, S. W. and Gower, S. T. 1991. 'FOREST–BGC, a general model of forest ecosystem processes for regional applications. II. Dynamic carbon allocation and nitrogen budgets', *Tree Physiol.*, **9**, 147–160.
- Running, S. W. and Hunt, E. R., Jr. 1993. 'Generalization of a forest ecosystem process model for other biomes, BIOME–BGC, and an application for global-scale models', in Ehleringer, J. R. and Field, C. B. (Eds.), *Scaling Physiological Processes: Leaf to Globe*. Academic Press, San Diego. pp. 141–158.
- Running, S. W., Nemani, R. R., and Hungerford, R. D. 1987. 'Extrapolation of synoptic meteorological data in mountainous terrain and its use for simulating forest evapotranspiration and photosynthesis', *Can. J. For. Res.*, **17**, 472–483.
- Running, S. W., Nemani, R. R., Peterson, D. L., Band, L. E., Potts, D. F., and Pierce, L. L. 1989. 'Mapping regional forest evapotranspiration and photosynthesis by coupling satellite data with ecosystems simulation', *Ecology*, **70**, 1090–1101.
- Sala, O., Jobbagy, E. G., Canadell, J., Ehleringer, J. R., Jackson, R. B., Mooney, J. A., Panuelo, J. M., and Schulze, E. D. 1996. 'Ecosystem rooting depth patterns and controls: a modeling approach', *Paper at 1996 Meeting of the Ecological Society of America, Providence, RI*.
- Sivapalan, M., Beven, K., and Wood, E. F. 1987. 'On hydrologic similarity 2. A scaled model of storm runoff production', *Wat. Resour. Res.*, **23**, 2266–2278.
- Vertessy, R. A., Hatton, T. J., Benyon, R. G., and Dawes, W. R. 1996. 'Long-term growth and water balance predictions for a mountain ash (*Eucalyptus regnans*) forest catchment subject to clear-felling and regeneration', *Tree Physiology*, **16**, 221–232.
- Wigmosta, M. S., Vail, L. W., and Lettenmaier, D. P. 1994. 'A distributed hydrology-vegetation model for complex terrain', *Water Resources Research*, **30**(6), 1665–1679.
- Wolock, D. M., Hornberger, G. M., Beven, K. J., and Campbell, W. G. 1989. 'The relationship of catchment topography and soil hydraulic characteristics to lake alkalinity in the northeastern United States', *Wat. Resour. Res.*, **25**, 829–837.